# High-Sensitivity Instantaneous Microwave Frequency Measurement Based on a Silicon Photonic Integrated Fano Resonator

Beibei Zhu, Weifeng Zhang, *Member, IEEE*, Shilong Pan, *Senior Member, IEEE, Senior Member, OSA*, and Jianping Yao, *Fellow, IEEE, Fellow, OSA*

*(Invited Paper)*

***Abstract*—Instantaneous frequency measurement (IFM) based on a silicon photonic Fano resonator with improved linearity and sensitivity is proposed and experimentally demonstrated. The Fano resonator has a steep edge in its spectral response, which is employed to translate the frequency information of a microwave signal to an optical power change. When comparing the optical powers at the output and input of the Fano resonator, a highly linear amplitude comparison function (ACF), which is used to estimate the microwave frequency is obtained. The key device in the system is the Fano resonator, which is realized by coupling a grating-based Fabry–Perot cavity resonant mode with an add-drop microring resonator mode, implemented on a silicon platform. The linearity of the ACF is characterized by its R-squared value which is calculated by fitting the ACF measurements with a linear function. In our experimental demonstration, an R-squared value as large as 0.99 is obtained. A frequency measurement range as large as 15 GHz with a resolution better than ±0.5 GHz is achieved. The use of the proposed IFM system to perform Brillouin frequency discrimination in a fiber-optic sensor for temperature measurement is demonstrated.**

***Index Terms*—Carrier-suppressed single sideband modulation, Fano resonance, instantaneous frequency measurements, microwave photonics, silicon photonics.**

## I. Introduction

INSTANTANEOUS frequency measurement (IFM) of a microwave or millimeter-wave signal is of great importance for applications in electronic warfare and cognitive radio systems and for high resolution sensor systems. In recent years, photonics-based techniques for IFM have been intensively investigated and numerous approaches have been proposed and demonstrated. The key advantages of performing IFM based on photonics include ultra-fast measurement speed, high accuracy, and large frequency measurement range [1], [2]. In general, photonics-based IFM techniques can be divided into three categories: frequency-to-microwave power mapping [3]–[8], frequency-to-optical power mapping [9]–[22], and frequency-to-time mapping [23]–[25].

For techniques based on frequency-to-microwave power mapping [3]–[8], a microwave signal with its frequency to be measured is first converted into an optical signal through electrical to optical conversion using an optical modulator, and then sent the modulated optical signal to a photonic processing module (a dispersive element or an optical filter), where a monotonic frequency-dependent microwave power penalty function in the optical domain is introduced. A photodetector (PD) is connected to the photonic processing module to convert the optical signal into a microwave signal. To make the measurement to be independent of the input power, two parallel channels which provide different, usually opposite frequency-dependent power penalty functions, are needed. The power ratio of the microwave signals from the two channels, called amplitude comparison function (ACF), is a function of the input microwave frequency. The major problem associated with these techniques is that high-frequency PDs and wideband microwave devices are needed, making the systems costly.

To avoid the use of expensive microwave devices, techniques based on frequency-to-optical power mapping were proposed and the ACF is the power ratio between the optical powers measured at the outputs of two optical paths [9]–[22]. The key component in such a system is a photonic processing module, such as an optical filter [9]–[16] or an optical mixing unit [17]–[22], to translate the frequency of an input microwave signal to an optical power change. In most of the IFM schemes based on frequency-to-optical power mapping, an optical filter with a sinusoidal spectral response is employed to perform frequency to power mapping, which leads to an ACF with very

Manuscript received July 30, 2018; revised October 31, 2018; accepted December 3, 2018. Date of publication December 5, 2018; date of current version May 1, 2019. This work was supported by the Natural Sciences and Engineering Council of Canada (NSERC). The work of B. Zhu was supported by a scholarship from the China Scholarship Council. *(Corresponding author: Jianping Yao.)*

B. Zhu is with the Microwave Photonics Research Laboratory, School of Electrical Engineering and Computer Science, University of Ottawa, Ottawa, ON K1N 6N5, Canada, and also with the College of Electronic and Information Engineering, Nanjing University of Aeronautics and Astronautics, Nanjing 210016, China.

W. Zhang and J. Yao are with the Microwave Photonics Research Laboratory, School of Electrical Engineering and Computer Science, University of Ottawa, Ottawa, ON K1N 6N5, Canada (e-mail: jpyao@uottawa.ca).

S. Pan is with the College of Electronic and Information Engineering, Nanjing University of Aeronautics and Astronautics, Nanjing 210016, China (e-mail: pans@nuaa.edu.cn).

Color versions of one or more of the figures in this paper are available online at http://ieeexplore.ieee.org.

Digital Object Identifier 10.1109/JLT.2018.2885224

poor linearity. For example, a Sagnac loop based filter with 50 GHz free spectral range (FSR) was used in [9]. The microwave signal with an unknown frequency was modulated on two optical carriers, one of which was set at a peak and the other at a valley of the filter spectral response. The power ratio of the two modulated signals, which is the ACF, is given by [9]

$$\mathrm{ACF} = \frac{1 - \cos\left(2\pi f_{RF}/\mathrm{FSR}\right)}{1 + \cos\left(2\pi f_{RF}/\mathrm{FSR}\right)} \tag{1}$$

where $f_{\mathrm{RF}}$ is the frequency to be measured. The R-square value is calculated to be 0.65806, which is very low, indicating a poor linearity.

For techniques based on frequency-to-time mapping [23]–[25], the frequency of an unknown microwave signal is converted into an electrical time delay using a dispersive time delay device [23] or a frequency shifting recirculating delay line (FS-RDL) [24], [25]. Since a dispersive element has a linear group delay and a FS-RDL has equal frequency shift per roundtrip time, these techniques can lead to a linear IFM system. However, the dispersion-based method has a relatively low resolution ($\sim$12.5 GHz) and a large measurement error (about $\pm$1.56 GHz). The FS-RDL-based method has a long response time, which may not be suitable for instantaneous frequency measurements.

To achieve an IFM system with a high linearity, high resolution, and short response time, a photonic processing module with a highly linear frequency response to perform frequency to power conversion is required. A linear ACF would ensure identical measurement sensitivity for an entire frequency measurement range, which is important for an IFM system to have a high and uniform measurement resolution and accuracy. For instance, a special FBG with two linear and complementary spectral slopes was applied to achieve a highly linear ACF [13]. A measurement range of 1–10 GHz and a measurement accuracy of $\pm$0.2 GHz were demonstrated [13].

Among the approaches [3]–[25], those reported in [7], [8], [14], [15], [18], [19], [22] were implemented based on integrated photonic devices. The size is smaller, the stability is better, the measurement latency is shorter, and the unit cost is lower. These make integrated IFM attractive for practical applications. However, those integrated solutions have poor linearity, making the measurement resolution not uniform over the frequency measurement range.

The performance of the integrated IFM techniques is summarized in Table I, in which the measurement range, measurement error and input power to the chip are considered. As can be seen the input power levels for all the approaches [7], [8], [14], [15], [18], [19], [22] were very high. For a practical IFM system, the input power from a receiver is usually very low. Thus, a solution to perform IFM with a lower input power is needed.

In this paper, we propose and experimentally demonstrate a novel approach to achieve IFM based on a silicon photonic integrated Fano resonator with high linearity, high sensitivity and low input power. The key device in the system is the Fano resonator which is implemented using a grating-based Fabry-Perot (FP) cavity-coupled add-drop microring resonator (MRR), where the resonant mode of the FP cavity interferes with the resonant mode of the MRR in transmission response to produce the Fano resonance. When an optical wave that carries a microwave signal is applied to the Fano resonator, the frequency information is converted to an optical power. By calculating the ratio between the optical powers at the input and the output ports of the Fano resonator, an ACF is obtained and the frequency of the microwave signal is measured. A proof-of-concept experiment is carried out. With only 0 dBm input power to the chip, a frequency measurement range as large as 15 GHz with a resolution better than $\pm$0.5 GHz is achieved. The use of the proposed approach for Brillouin frequency discrimination in a fiber-optic sensor for high resolution temperature measurement is studied and demonstrated. A measurement sensitivity as large as 1.24 MHz/°C is achieved.

TABLE I
PERFORMANCE OF IFM TECHNIQUES BASED ON INTEGRATED PHOTONICS

| Techniques | Measurement range (GHz) | Measurement error (GHz) | Input Power (dBm) |
|---|---|---|---|
| SBS [7] | 0-38 | ±0.001 | 20 |
| FBG [8] | 0-32 | ±2.5 | 10 |
| PM-IM conversion [14] | 0.5-4 | ±0.094 | 20 |
| Ring-assisted MZI [15] | 5-15 | ±0.2 | 12 |
| Nonlinear effect [18] | >2.5×10$^3$ | - | 22 |
| Nonlinear effect [19] | 640 Gbit/s | - | 14 |
| Nonlinear effect [22] | 0-40 | ±0.318 | >20 |

## II. PRINCIPLE

The schematic of the proposed system using a Fano resonator for instantaneous microwave frequency measurement is shown in Fig. 1. A continuous wave (CW) optical carrier ($\lambda_c$) is modulated by a microwave signal with its frequency to be measured at a Mach-Zehnder modulator (MZM) that is biased at the minimum transmission point (MITP) to generate a double-sideband modulated signal with suppressed carrier. After filtering out the lower sideband using an optical bandpass filter (OBPF), a carrier-suppressed single-sideband (CS-SSB) signal is achieved and launched into the silicon chip via an optical circulator (OC). Part of the CS-SSB signal is transmitted through the Fano resonator while the other part of the CS-SSB signal is reflected by the grating. The ACF, defined as the power ratio between the transmitted and reflected average optical powers, is given

$$\mathrm{ACF}\left(\lambda\right) = \frac{P_{\mathrm{TX}}\left(\lambda\right)}{P_{\mathrm{RX}}\left(\lambda\right)} \tag{2}$$

Since the frequency of the microwave signal has a unique relationship with the ACF, once the ACF value is known, the frequency of the microwave signal is measured. Note that the optical powers rather than the microwave powers are measured, thus no high speed PDs are needed.

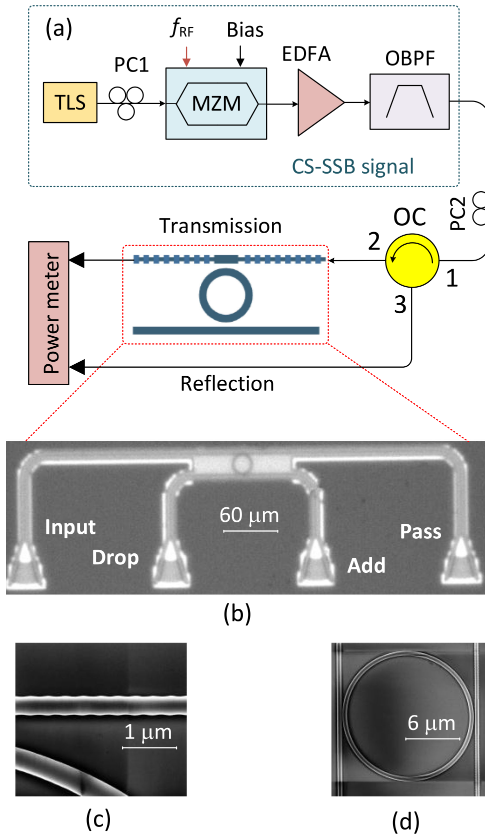


Fig. 1. (a) Schematic diagram of the proposed IFM system. (b) Image of the fabricated Fano resonator obtained from a microscope camera. (c) The SEM image of the Bragg grating. (d) The SEM image of the MRR. CS-SSB: carrier-suppressed single-sideband; TLS: tunable laser source; PC: polarization controller; MZM: Mach-Zehnder modulator; EDFA: erbium-doped fiber amplifier; OBPF: optical bandpass filter; OC: optical circulator.

## III. Frequency Measurement of a Microwave Signal

A proof-of-concept experiment is carried out based on the setup in Fig. 1. An optical carrier emitting at 1556.2 nm with a power of 8 dBm is generated from a tunable laser source (TLS, Anritsu MG9638A), which is then modulated by a microwave signal from a microwave source (Agilent E8254A) at a 20-GHz MZM (JDS Uniphase, Model 10026465). The MZM is biased at the MITP and the microwave signal is amplified by an RF amplifier (MultiLink modulator driver MTC5515-751) by 20 dB. Then, the carrier-suppressed double-sideband (CS-DSB) signal is amplified using an erbium-doped fiber amplifier (EDFA, Nortel Inc.) before introduced into the OBPF (Finisar, Waveshaper 4000 s). The lower sideband (LSB) is selected and launched into the chip and the input power is kept around 0 dBm since the EDFA works in a constant output power mode (Automatic Power Control, APC). The total loss of the chip is 13.6 dB. The optical powers at the transmission and reflection ports are simultaneously measured by a two-channel optical power meter (HP 8152A). Since the Fano resonator will experience a spectral shift when the temperature changes, accurate and stable temperature control (TEC, ILX Lightwave LDT-5910B) is employed to make the temperature of the chip fixed at 23 °C. Thanks to the stable environmental temperature and low input power to the chip, the TEC controller can easily make the temperature stabilized with a temperature variation smaller than 0.01 °C during the process of the experiment and the power ratio of the two channels is calculated and recorded. Since the two parallel channels are experiencing the same environmental fluctuations, the impact of the temperature change to the ACF is small and can be neglected.

The transmission and reflection spectral responses of the Fano resonator, which was first reported by us in [26] are measured by an optical vector analyzer (LUNA OVA CTe) and shown in Fig. 2(a) and (b). A zoom-in view of the region around the Fano resonance is shown in Fig. 2(c) and (d). The ACF is calculated using (2), which is shown in Fig. 2(e). A zoom-in view of the linear region of the ACF is shown in Fig. 2(f) covering a frequency range of 15 GHz. The R-square for the linear region is calculated which is 0.98658.

Fig. 3 shows the measured microwave frequencies when the output powers from the microwave source are set at −5 dBm, 0 dBm and 5 dBm. The frequency tuning range is from 3 to 18 GHz, which cannot be higher due to the limited bandwidth of the 20 GHz MZM. The solid line shows the actual ACF of the system. The measurement errors which are the difference between the measured ACF values and the actual ACF values are shown in Fig. 4. The measurement errors are smaller than ±0.5 GHz over the entire frequency measurement range from 3 to 18 GHz. The standard deviations of the errors for the three power levels are calculated to be 0.1331, 0.1227, and 0.1625 (0.1142 without counting the first two points which have higher errors). As can be seen, a higher input power will lead to smaller measurement errors. A higher microwave power results in a higher modulation index so that the signal-to-noise ratio (SNR) of the modulated optical signal is higher after amplification. The measurement errors for lower frequencies are higher when the signal power is 5 dBm. This is because the high order sidebands are stronger which are harder to be removed by the optical bandpass filter.

The approach is effective for the measurement of a single-frequency microwave signal. If a modulated microwave signal is applied to the input of the IFM system, each frequency component of the input microwave signal will be mapped to a corresponding optical power and the output power will be the sum of all the optical powers. Since an R-squared value as large as 0.99 is obtained in the proposed IFM system, the power-frequency relation is highly linear and the measurement result will be a linear combination of the frequencies, which will cause measurement errors. Taking a double-sideband plus carrier (DSB+C) signal as an example, if the carrier frequency is 10 GHz, and each of the two sidebands has a power that is 5% or 10% of the power of the microwave carrier, we calculate the measurement errors as a function of the sideband frequency, as shown in Fig. 5. As can be seen, the measurement error decreases as the frequency of the sidebands and the sideband-to-carrier power ratio decrease. If the two sidebands are separated from the microwave carrier by 1 GHz, the frequency measurement error is 0.2 GHz (or 2%) or 0.4 GHz (or 4%).

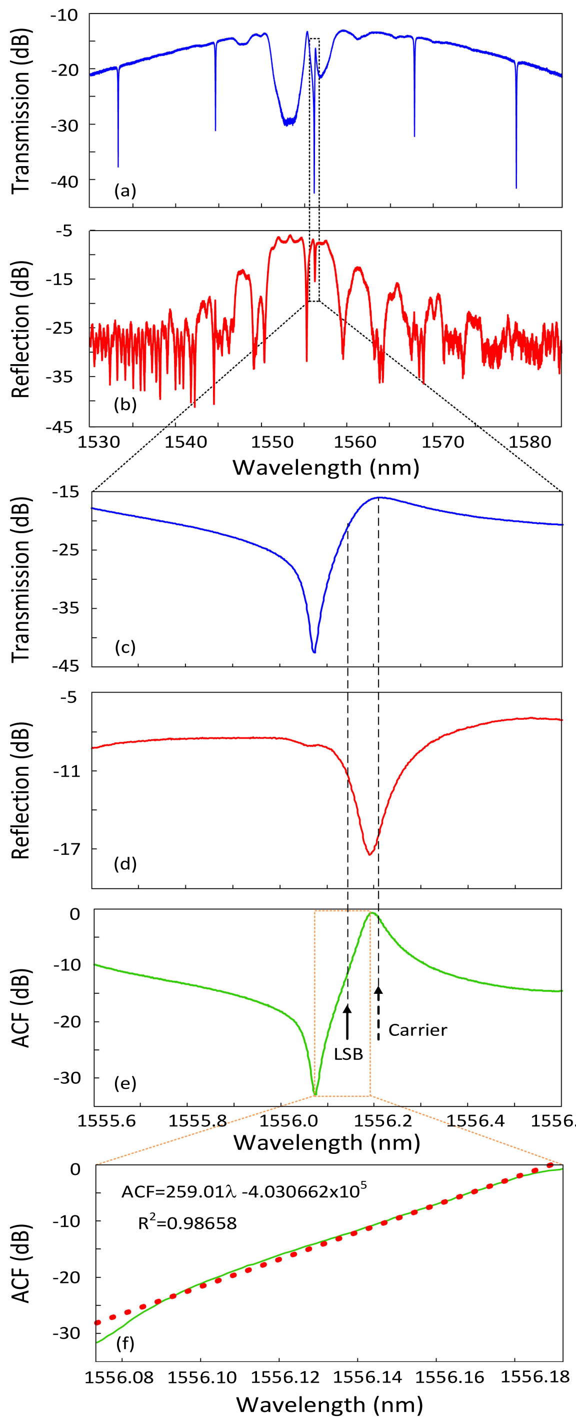


Fig. 2. (a) Transmission spectral response of the device, (b) reflection spectral response of the device, (c) and (d) zoom-in views of the region around the Fano resonance, (e) ACF, and (f) a zoom-in view of the linear region of the ACF with linear fitting.

## IV. Frequency Discrimination in a Brillouin Fiber Sensing System

Distributed Brillouin-based optical fiber sensors are widely used in civil infrastructure and power supply systems to monitor the temperature and strain variations along the sensing fibers [27]. High speed and high resolution interrogation of

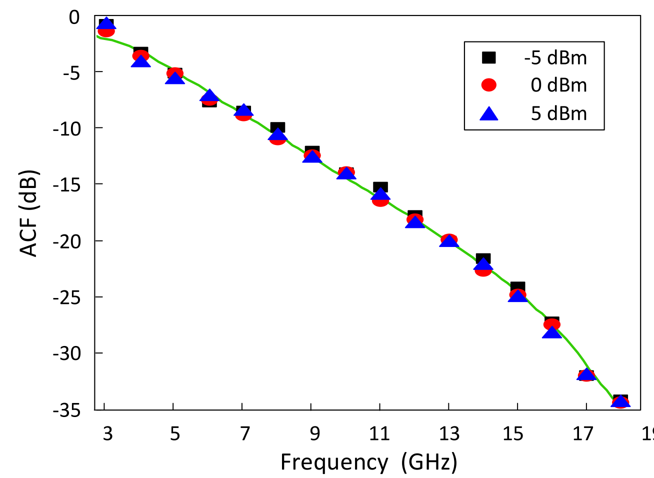


Fig. 3. Measured microwave frequencies when the input powers of the unknown microwave signal are −5 dBm, 0 dBm and 5 dBm.

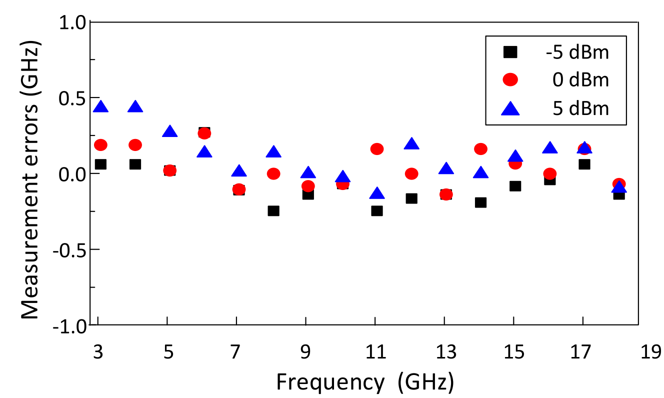


Fig. 4. Measurement errors when the input powers of the microwave signal are at −5 dBm, 0 dBm and 5 dBm.

the Brillouin frequency shift (BFS) of such a sensor is a key procedure to ensure a high performance temperature and strain sensing [28], [29]. Thanks to the high speed and high linearity, the proposed IFM system is a good candidate to achieve real-time BFS discrimination in a Brillouin fiber-optic sensing system.

Fig. 6 shows the experimental setup to use the proposed IFM technique to interrogate a Brillouin sensor. A CW light emitted from a TLS (Anritsu MG9638A) is amplified by an EDFA (Nortel) to 15.8 dBm and then launched into a 10-km single-mode fiber (SMF) through an optical circulator (OC1) as a pump source. Due to stimulated Brillouin scattering, a Brillouin gain spectrum at a longer wavelength is resulted, as shown in Fig. 7. A peak at the same wavelength as the pump wavelength due to Rayleigh scattering is seen, which is removed by an OBPF (Finisar, Waveshaper 4000s), as also shown in Fig. 7. The Brillouin gain spectrum is introduced into the IFM chip through a second OC (OC2). By detecting the transmission and reflection powers, the optical frequency of the Brillouin gain spectrum is estimated. To evaluate its performance as a temperature sensor, in the experiment we change the temperature of the SMF from 75 °C to 25 °C, the values of the BFS

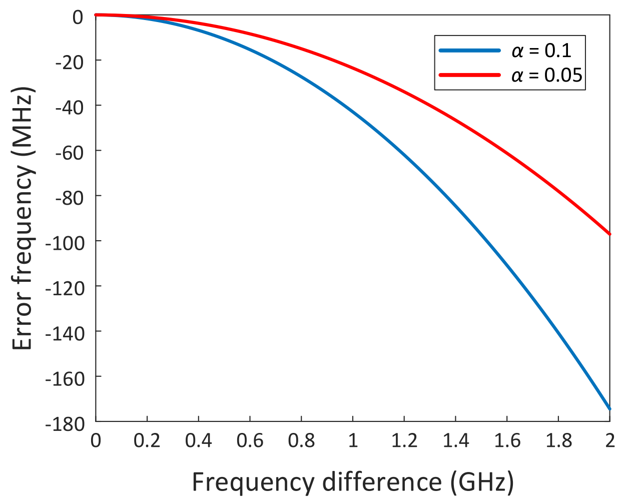


Fig. 5. Measurement errors of a DSB+C signal with 10 GHz microwave carrier when the sideband-to-carrier power ratios are 5% and 10%.

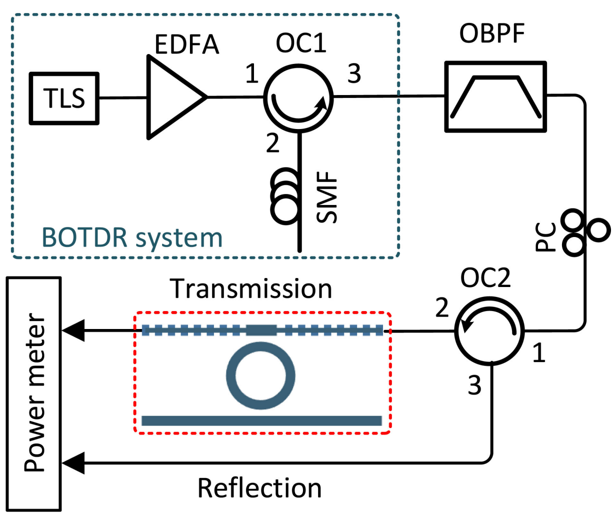


Fig. 6. Experiment setup of the proposed microwave frequency measurement system. BOTDR: Brillouin optical time domain reflectometry; SMF: single-mode fiber.

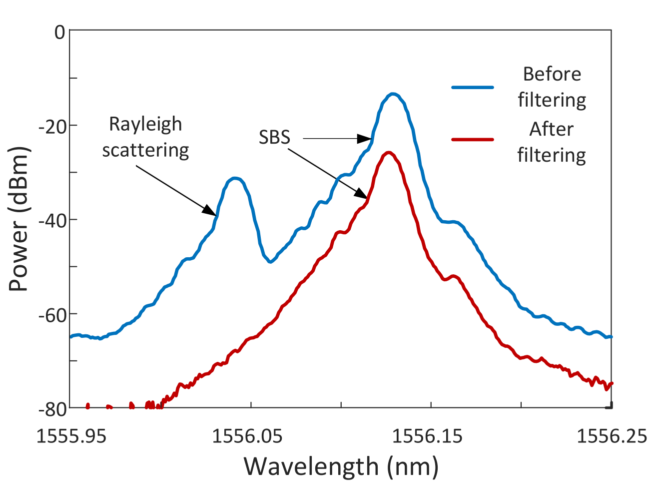


Fig. 7. Optical spectra before and after optical filtering.

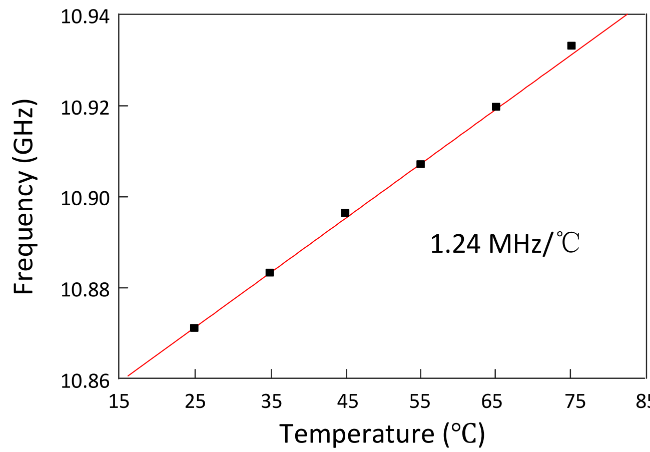


Fig. 8. Brillouin frequency shift as a function of the temperature change of the SMF.

are measured. As can be seen from Fig. 8 the values are decreased with a fitted slope of 1.24 MHz/°C. The measurement errors are within ±1.64 MHz, which are mainly caused by the nonuniformity of the temperature distribution in such a long fiber as well as the strain variations caused by the temperature change.

Note that if the CW light source and the two-channel optical power meter are replaced by an optical pulse source and two low-speed PDs, the sensor can be used for high speed and high resolution distributed temperature sensing. For practical implementations, temperature control of the chip can be used to control the temperature of the chip in real time so that the measurement errors would be further reduced.

## V. Conclusion

A novel approach to implement instantaneous frequency measurement based on a silicon photonic Fano resonator with high linearity, high sensitivity and low input power was proposed and experimentally demonstrated, for the first time, to the best of our knowledge. The Fano resonance was generated by coupling a grating-based FP cavity with an MRR. When the resonant mode of the FP cavity interfered with the resonant mode of the MRR, an asymmetric Fano response with a steep edge in its spectral response was realized, which was used to convert the frequency of a microwave signal to an optical power change. By comparing the optical powers at the output and the input ports of the Fano resonator, an ACF with high linearity was obtained. An experiment was performed. The R-squared value of the measured ACF was 0.99 while is very high confirming a good linearity of the ACF. The input power to the chip was about 0 dBm, which was low. A frequency measurement range as large as 15 GHz with a resolution better than ±0.5 GHz was achieved. The proposed IFM system was also used for Brillouin frequency discrimination in a fiber-optic sensor for temperature measurement. A linear dependence between the Brillouin frequency shift and the temperature variations was measured to be 1.24 MHz/°C with measurement errors within ±1.64 MHz.

## References


[1] X. Zou, B. Lu, W. Pan, L. Yan, A. Stöhr, and J. Yao, "Photonics for microwave measurements," *Laser Photon. Rev.*, vol. 10, no. 5, pp. 711–734, Sep. 2016.

[2] S. Pan and J. Yao, "Photonics-based broadband microwave measurement," *J. Lightw. Technol.*, vol. 35, no. 16, pp. 3498–3513, Aug. 2017.

[3] X. Zhang, H. Chi, X. Zhang, S. Zheng, X. Jin, and J. Yao, "Instantaneous microwave frequency measurement using an optical phase modulator," *IEEE Microw. Wireless Compon. Lett.*, vol. 19, no. 6, pp. 422–424, Jun. 2009.

[4] X. Zou, S. Pan, and J. Yao, "Instantaneous microwave frequency measurement with improved measurement range and resolution based on simultaneous phase modulation and intensity modulation," *J. Lightw. Technol.*, vol. 27, no. 23, pp. 5314–5320, Dec. 2009.

[5] M. Attygalle and D. B. Hunter, "Improved photonic technique for broadband radio-frequency measurement," *IEEE Photon. Technol. Lett.*, vol. 21, no. 4, pp. 206–208, Feb. 2009.

[6] H. Emami and M. Ashourian, "Improved dynamic range microwave photonic instantaneous frequency measurement based on four-wavemixing," *IEEE Trans. Microw. Theory Techn.*, vol. 62, no. 10, pp. 2462–2470, Oct. 2014.

[7] H. Jiang *et al.*, "Wide-range, high-precision multiple microwave frequency measurement using a chip-based photonic Brillouin filter," *Optica*, vol. 3, no. 1, pp. 30–34, Jan. 2016.

[8] M. Burla, X. Wang, M. Li, L. Chrostowski, and J. Azaña, "Wideband dynamic microwave frequency identification system using a low-power ultracompact silicon photonic chip," *Nature Commun.*, vol. 7, Sep. 2016, Art. no. 13004.

[9] H. Chi, X. Zou, and J. Yao, "An approach to the measurement of microwave frequency based on optical power monitoring," *IEEE Photon. Technol. Lett.*, vol. 20, no. 14, pp. 1249–1251, Jul. 2008.

[10] X. Zou, H. Chi, and J. Yao, "Microwave frequency measurement based on optical power monitoring using a complementary optical filter pair," *IEEE Trans. Microw. Theory Techn.*, vol. 57, no. 2, pp. 505–511, Feb. 2009.

[11] X. Zou, W. Pan, B. Luo, and L. Yan, "Full-scale phase demodulation approach for photonic instantaneous frequency measurement," *Opt. Lett.*, vol. 35, no. 16, pp. 2747–2749, Aug. 2010.

[12] S. Pan, J. Fu, and J. Yao, "Photonic approach to the simultaneous measurement of the frequency, amplitude, pulse width, and time of arrival of a microwave signal," *Opt. Lett.*, vol. 37, no. 1, pp. 7–9, Jan. 2012.

[13] Z. Li, C. Wang, M. Li, H. Chi, X. Zhang, and J. Yao, "Instantaneous microwave frequency measurement using a special fiber Bragg grating, " *IEEE Microw. Wireless Compon. Lett.*, vol. 21, no. 1, pp. 52–54, Jan. 2011.

[14] D. Marpaung, "On-chip photonic-assisted instantaneous microwave frequency measurement system," *IEEE Photon. Technol. Lett.*, vol. 25, no. 9, pp. 837–840, May 2013.

[15] J. S. Fandiño and P. Muñoz, "Photonics-based microwave frequency measurement using a double-sideband suppressed-carrier modulation and an InP integrated ring-assisted Mach–Zehnder interferometer filter," *Opt. Lett.*, vol. 38, no. 21, pp. 4316–4319, Nov. 2013.

[16] L. Liu *et al.*, "Photonic measurement of microwave frequency using a silicon microdisk resonator," *Opt. Commun.*, vol. 335, pp. 266–270, Jan. 2015.

[17] H. Emami, N. Sarkhosh, L. Bui, and A. Mitchell, "Amplitude independent RF instantaneous frequency measurement system using photonic Hilbert transform," *Opt. Exp.*, vol. 16, no. 18, pp. 13707–13712, Sep. 2008.

[18] M. Pelusi *et al.*, "Photonic-chip-based radio-frequency spectrum analyser with terahertz bandwidth," *Nature Photon.*, vol. 3, no. 1, pp. 139–143, Jan. 2009.

[19] B. Corcoran *et al.*, "Silicon nanowire based radio-frequency spectrum analyzer," *Opt. Express*, vol. 18, no. 19, pp. 20190–20200, Sep. 2010.

[20] L. Bui, N. Sarkhosh, and A. Mitchell, "Photonic instantaneous frequency measurement: Parallel simultaneous implementations in a single highly nonlinear fiber," *IEEE Photon. J.*, vol. 2, no. 5, pp. 915–925, Oct. 2011.

[21] D. Q. Feng, H. Xie, L. F. Qian, Q. H. Bai, and J. Q. Sun, "Photonic approach for microwave frequency measurement with adjustable measurement range and resolution using birefringence effect in highly non-linear fiber," *Opt. Express*, vol. 23, no. 13, pp. 17613–17621, Jun. 2015.

[22] M. Pagani *et al.*, "Low-error and broadband microwave frequency measurement in a silicon chip," *Optica*, vol. 2, no. 8, pp. 751–756, Aug. 2015.

[23] L. V. Nguyen, "Microwave photonic technique for frequency measurement of simultaneous signals," *IEEE Photon. Technol. Lett.*, vol. 21, no. 10, pp. 642–644, May 2009.

[24] T. A. Nguyen, E. H.W. Chan, and R. A. Minasian, "Instantaneous high resolution multiple-frequency measurement system based on frequency-to-time mapping technique," *Opt. Lett.*, vol. 39, no. 8, pp. 2419–2422, Apr. 2014.

[25] T. A. Nguyen, E. H.W. Chan, and R. A. Minasian, "Photonic multiple frequency measurement using a frequency shifting recirculating delay line structure," *J. Lightw. Technol.*, vol. 32, no. 20, pp. 3831–3838, Oct. 2014.

[26] W. Zhang and J. P. Yao, "Optically tunable Fano resonance in a grating-based Fabry-Perot cavity-coupled microring resonator on a silicon chip," *Opt. Lett.*, vol. 41, no. 11, pp. 2474–2477, Jun. 2016.

[27] T. Horiguchi, K. Shimizu, T. Kurashima, M. Tateda, and Y. Koyamada, "Development of a distributed sensing technique using Brillouin scattering," *J. Lightw. Technol.*, vol. 13, no. 7, pp. 1296–1302, Jul. 1995.

[28] X. Bao and L. Chen, "Recent progress in Brillouin scattering based fiber sensors," *Sensors*, vol. 11, no. 4, pp. 4152–4187, Apr. 2011.

[29] D. Zhou *et al.*, "Single-shot BOTDA based on an optical chirp chain probe wave for distributed ultrafast measurement," *Light Sci. Appl.*, vol. 7, no. 1, Jul. 2018, Art. no. 32.



**Beibei Zhu** received the B.S. degree in 2013 from Nanjing University of Aeronautics and Astronautics, Nanjing, China, where she is currently working toward the Ph.D. degree at the Key Laboratory of Radar Imaging and Microwave Photonics and the Ministry of Education. She has been a visiting student with the Microwave Photonics Research Laboratory, School of Electrical Engineering and Computer Science, University of Ottawa, Ottawa, ON, Canada, since September 2017.

Her current research interests include microwave photonic measurement techniques and applications.

**Weifeng Zhang** (S'12–M'17) received the B.Eng. degree in electronic science and technology from Xi'an Jiaotong University, Xi'an, China, in 2008, the M.A.Sc. degree in electrical engineering from the Politecnico di Torino, Torino, Italy, in 2011, and the Ph.D. degree in electrical engineering from the University of Ottawa, Ottawa, ON, Canada, in 2017. He is currently a Postdoctoral Fellow with the Microwave Photonics Research Laboratory, School of Electrical Engineering and Computer Science, University of Ottawa.

His current research interests include silicon photonics and its applications in microwave photonics.

**Shilong Pan** (S'06–M'09–SM'13) received the B.S. and Ph.D. degrees in electronics engineering from Tsinghua University, Beijing, China, in 2004 and 2008, respectively. From 2008 to 2010, he was a "Vision 2010" Postdoctoral Research Fellow with the Microwave Photonics Research Laboratory, University of Ottawa, Canada. He joined the College of Electronic and Information Engineering, Nanjing University of Aeronautics and Astronautics, China, in 2010, where he is currently a Full Professor and an Executive Director with the Key Laboratory of Radar Imaging and Microwave Photonics, the Ministry of Education.

His research has focused on microwave photonics, which includes optical generation and processing of microwave signals, analog photonic links, photonic microwave measurement, and integrated microwave photonics. He has authored or coauthored over 380 research papers, including more than 200 papers in peer-reviewed journals and 180 papers in conference proceedings.

Dr. Pan is a Fellow of IET and a Senior Member of OSA and SPIE. He was the recipient of an OSA outstanding reviewer award in 2015 and a top reviewer of IEEE/OSA Journal of Lightwave Technology in 2016. He was also the recipient of the Excellent Young Scholars Award of the National Natural Science Foundation of China in 2014, and the Scientific and Technological Innovation Leading Talents Award of the National Ten Thousand Plan in 2018. He is currently an Associate Editor for *Electronics Letters*, a Topical Editor for *Chinese Optics Letters*, and a Technical Committee member for IEEE MTT-3 Microwave Photonics. He is a Steering Committee Member of IEEE International Topical Meeting on Microwave Photonics, and International Conference on Optical Communications and Networks. He has also served as a Chair for a number of international conferences, symposia, and workshops, including the TPC Chair of the International Conference on Optical Communications and Networks in 2015, TPC Cochair of IEEE International Topical Meeting on Microwave Photonics in 2017, TPC Chair of the high-speed and broadband wireless technologies subcommittee of the IEEE Radio Wireless Symposium in 2013, 2014, and 2016, TPC subcommittee Chair of the OptoElectronics and Communication Conference in 2015, TPC subcommittee Cochair of CLEO Pacific Rim in 2018, International Conference on Information Optics and Photonics in 2018, and the Chair of the microwave photonics for broadband measurement workshop of International Microwave Symposium in 2015.

**Jianping Yao** (M'99–SM'01–F'12) received the Ph.D. degree in electrical engineering from the Université de Toulon et du Var, France, in December 1997. He is a Distinguished University Professor and University Research Chair with the School of Electrical Engineering and Computer Science, University of Ottawa, Ottawa, ON, Canada. From 1998 to 2001, he was with the School of Electrical and Electronic Engineering, Nanyang Technological University (NTU), Singapore, as an Assistant Professor. In December 2001, he joined the School of Electrical Engineering and Computer Science, University of Ottawa, as an Assistant Professor, where he was promoted to Associate Professor in May 2003, and Full Professor in May 2006. He was appointed University Research Chair in Microwave Photonics in 2007. In June 2016, he was conferred the title of Distinguished University Professor of the University of Ottawa. From July 2007 to June 2010 and July 2013 to June 2016, he served as Director of the Ottawa-Carleton Institute for Electrical and Computer Engineering. He has authored or coauthored over 560 research papers including over 330 papers in peer-reviewed journals and over 230 papers in conference proceedings.

Dr. Yao is a registered Professional Engineer of Ontario. He is a Fellow of the Optical Society of America, the Canadian Academy of Engineering, and the Royal Society of Canada. He was the recipient of the 2005 International Creative Research Award of the University of Ottawa, the 2007 George S. Glinski Award for Excellence in Research, Natural Sciences and Engineering Research Council of Canada Discovery Accelerator Supplements Award in 2008, and the Award for Excellence in Research 2017–2018 of the University of Ottawa. He was selected to receive an inaugural OSA Outstanding Reviewer Award in 2012 and was one of the top ten reviewers of IEEE/OSA JOURNAL OF LIGHTWAVE TECHNOLOGY 2015–2016. He was an IEEE MTT-S Distinguished Microwave Lecturer for 2013–2015. He is Editor-in-Chief for IEEE PHOTONICS TECHNOLOGY LETTERS, a Topical Editor for *Optics Letters*, an Associate Editor for *Science Bulletin*, a Steering Committee Member for IEEE/OSA JOURNAL OF LIGHTWAVE TECHNOLOGY, and an Advisory Editorial Board Member for *Optics Communications*. He was a Guest Editor of a Focus Issue on Microwave Photonics in *Optics Express* in 2013, a Lead Editor of a Feature Issue on Microwave Photonics in *Photonics Research* in 2014, and a Guest Editor of a special issue on Microwave Photonics in IEEE/OSA JOURNAL OF LIGHTWAVE TECHNOLOGY in 2018. He currently serves as the Chair of the IEEE Photonics Ottawa Chapter, and is the Technical Committee Chair of IEEE MTT-3 Microwave Photonics. He was a member of the European Research Council Consolidator Grant Panel in 2016, the Qualitative Evaluation Panel in 2017, and a member of the National Science Foundation Career Awards Panel in 2016. He has also served as a Chair of a number of international conferences, symposia, and workshops, including the Vice Technical Program Committee (TPC) Chair of the 2007 IEEE Topical Meeting on Microwave Photonics, TPC Cochair of the 2009 and 2010 Asia-Pacific Microwave Photonics Conference, TPC Chair of the high-speed and broadband wireless technologies subcommittee of the IEEE Radio Wireless Symposium 2009–2012, TPC Chair of the microwave photonics subcommittee of the IEEE Photonics Society Annual Meeting 2009, TPC Chair of the 2010 IEEE Topical Meeting on Microwave Photonics, General Cochair of the 2011 IEEE Topical Meeting on Microwave Photonics, TPC Co-Chair of the 2014 IEEE Topical Meetings on Microwave Photonics, and General Cochair of the 2015 and 2017 IEEE Topical Meeting on Microwave Photonics. He has also served as a committee member for a number of international conferences, such as IPC, OFC, BGPP, and MWP.